Multichannel Blind Deconvolution of Spatially Misaligned Images

Filip Šroubek and Jan Flusser, *Senior Member, IEEE*

***Abstract*— Existing multichannel blind restoration techniques are prone to noise, assume perfect spatial alignment of channels and a correct estimation of blur size. We develop an alternating minimization scheme based on a maximum a posterior estimation with a priori distribution of blurs derived from the multichannel framework and a priori distribution of original images defined by the total variation semi-norm. This stochastic approach enables us to recover the blurs and the original image from channels severely corrupted by noise. We observe that the exact knowledge of the blur size is not necessary and we prove that translation misregistration up to a certain extent can be automatically removed in the restoration process.**

***Index Terms*— multichannel blind deconvolution, image restoration, total variation, subspace methods, MAP estimator, conjugate gradient**

I. Introduction

In many applications, such as microscopy imaging, remote sensing and astronomical imaging, observed images are degraded by distortion. Examples of most common distortions are atmospheric turbulence, relative motion between a camera and an object or wrong focus. Restoration of the degraded images is generally a necessary step that precedes any other image processing or segmentation tasks.

First, a proper mathematical model that simulates the acquisition system is required. Images may be regarded as either deterministic or stochastic signals, blurred by linear or nonlinear processes and corrupted with additive or multiplicative noise. Several constraints on the degradation and the original image were proposed and many different restoration algorithms were analyzed in the literature; see e.g. [1]. In the sequel, we adopt a linear filter model with additive uncorrelated noise, i.e.

$$z(x) = (h * u)(x) + n(x)\,,$$

where z, h, u and n are the degraded image, blur, original image and noise, respectively, and $*$ denotes convolution. This model accurately describes many common degradations and that justifies its frequent use.

The amount of a priori information about the degradation, like the size or shape of blurs and the noise level, significantly influences the success of restoration. When the blur function is known, many conventional approaches have been developed to compensate for the distortion. Such problems are solvable except at spatial frequencies where the Fourier transform of the blur function is zero or close to zero, which is a phenomenon that occurs almost surely. We therefore face an ill-posed problem that calls for regularization. When the blur is unknown, we talk about *blind image restoration*. Blind image restoration is extensively studied and many techniques have been proposed for its solution [2]. Most of the methods are iterative or recursive. They involve regularization terms based on any available a priori information which assure various statistical properties of the image and constrains the estimated image and/or restoration filter. As in the nonblind case, regularization is required to improve stability. Probably the most successful regularization approach is based on the total variation semi-norm [3]. Minimization of total variation preserves edges and fine details in the image and it was first applied to image denoising and later on to restoration. Nevertheless, since the blind case is strongly ill-posed, all the methods suffer from convergence and stability problems.

There are some applications, where several blurred versions of the same original image are observed through different acquisition channels. Adopting the above model, we write

$$z_k(x) = (h_k * u)(x) + n_k(x),\ k = 1, \ldots, K\,,$$

where K is the number of channels. Restoring the original image in this scenario is called *multichannel restoration* (MC). Examples of such multichannel measuring processes are common, e.g., in remote sensing and astronomy, where the same scene is observed at different time instants through a time-varying inhomogeneous medium such as the atmosphere; in confocal microscopy, where images of the same sample are acquired at different focusing lengths; or in broadband imaging through a physically stable medium but which has a different transfer function at different frequencies. Nonblind MC restoration is potentially free of the problems arising from the zeros of blurs. The lack of information from one blur in one frequency is supplemented by the information at the same frequency from others. Intuitively, one may expect that the blind restoration problem is also simplified by the availability of different channels. Two classes of multichannel blind image restoration algorithms exist. Extensions of singlechannel blind restoration approaches form the first class, but since they suffer from similar drawbacks as their singlechannel counterparts, they are of not much interest. The other class consists of intrinsic multichannel approaches, which evolved primarily from multichannel one-dimensional signal estimation methods and will be considered here.

The intrinsic multichannel algorithms basically come in three flavors. Harikumar et al. [4] proposed an indirect algorithm, which first estimates the blur functions and then

Financial support of this research was provided by the Grant Agency of the Czech Republic under the project No. 102/00/1711.

Filip Šroubek and Jan Flusser are with the Institute of Information Theory and Automation, Academy of Sciences of the Czech Republic, Pod vodárenskou věží 4, 182 08 Prague 8, Czech Republic, E-mail: {sroubekf,flusser}@utia.cas.cz

recovers the original image by standard nonblind methods. The blur functions are equal to the minimum eigenvector of a special matrix constructed by the blurred images. Necessary assumptions for perfect recovery of the blur functions are noise-free environment and channel coprimeness, i.e. a scalar constant is the only common factor of the blurs. Giannakis et al.[5] (and at the same time Harikumar et al. [6]) developed another indirect algorithm based on Bezout's identity of coprime polynomials which finds restoration filters and by convolving the filters with the observed images recovers the original image. Both algorithms are vulnerable to noise and even for a moderate noise level restoration may break down. In the latter case, noise amplification can be attenuated to a certain extent by increasing the restoration filter order, which comes at the expense of deblurring. Pai et al. [7], [8] proposed two direct multichannel restoration algorithms that, contrary to the previous two indirect algorithms, estimate directly the original image from the null space or from the range of a special matrix. In noisy cases, the direct algorithms are more stable than the indirect ones. Nevertheless, all the algorithms lack the necessary robustness since they do not include any noise assumptions in their derivation and miss regularization terms. Recently, we have proposed an iterative MC algorithm [9] that performs well even on noisy images. It is based on least-squares deconvolution by anisotropic regularization of the image and between-channel regularization of the blurs.

All the above mentioned intrinsic multichannel algorithms assume that the size of the blurs is known or can be correctly estimated, and that the channel outputs are spatially aligned (*registered*). These assumptions are seldom true in real applications and, to our knowledge, their impact have not yet been considered in previous works dedicated to multichannel restoration. Present techniques assume that the channels are correctly registered and if not they require a preprocessing step, which registers the channels.

In this paper, we address the issues of robustness, blur size and misregistration. Exploiting the stochastic model and Bayes' rule in Section III, we express the a posteriori probability of the original image in terms of the conditional probability and two a priori probabilities, which are derived from properties of bounded variation functions and from the multichannel framework. An alternating minimization (AM) algorithm as a solution to a maximum a posteriori probability (MAP) estimator is also given here. In Section IV, we examine the minimization algorithm for its ability to alleviate the blur-oversized problem and demonstrate its convergence properties. We illustrate that the channel misalignment can be perfectly neutralized by properly oversizing the blur support in Section V.

II. Notation

We use the following conventions throughout the paper.

$\mathbb{N}^2$	2D space of integers
$u : \mathbb{N}^2 \to \mathbb{R}$	image function with a finite rectangular support
$S_u \equiv (S_u^1, S_u^2)$	support size of the image u
$x = (i, j) \in \mathbb{N}^2$	position at the i-th row and the j-th column in the image
$u(x) \equiv u(i, j)$	image value at the position x
$\mathbf{u}$	$\equiv [u(1,1), u(2,1), \ldots, u(S_u^1, 1), u(1,2), \ldots, u(S_u^1, S_u^2)]^T$ image column vector, lowercase bold letters
$\mathbf{C}$	matrix, uppercase bold letters
$\|\cdot\|$	l^2 norm
$\det(\cdot)$	matrix determinant
$\mathrm{Tr}(\cdot)$	trace of a square matrix
$E\{\cdot\}$	expected value
$\mathcal{F}\{\cdot\}$	discrete 2D Fourier transform

We endow the vector space $\mathbb{N}^2$ with operators

"+" and "−"	defined in a standard way
$(i, j) + k$	abbreviated form for $(i, j) + (k, k)$
$\prod(i, j)$	$\equiv ij$
$(i, j) < (k, l)$	$\equiv \{i < k \wedge j < l\}$ and similarly other binary relations ">", "=", etc.

For our next discussion, it is necessary to define convolution with a variable output support in matrix-vector notation. We follow the definition in [4]. Let $u(x)$ and $v(y)$ be two images with support $1 \le x \le S_u$ and $1 \le y \le S_v = (s_1, s_2)$, respectively, and $B = (b_1, b_2)$, $T = (t_1, t_2)$, $B \le T$. We separate v column-wise and address individual columns as $v_1, \ldots, v_{s_2}$. We denote by $\mathbf{C}_{S_v}^{B,T}\{u\}$ a Toeplitz-block-Toeplitz matrix of size $\prod(T-B+1) \times \prod S_v$ such that the concatenated result of convolution $\sum_{B \le x \le T} u(y - x)v(x)$ is equal to $\mathbf{C}_{S_v}^{B,T}\{u\}\mathbf{v}$. This is given by

$$\mathbf{C}_{S_v}^{B,T}\{u\} = \underbrace{\begin{pmatrix} \mathbf{C}_{s_1}^{b_1,t_1}\{v_{b_2}\} & \ldots & \mathbf{C}_{s_1}^{b_1,t_1}\{v_{b_2-s_2+1}\} \\ \mathbf{C}_{s_1}^{b_1,t_1}\{v_{b_2+1}\} & \ldots & \mathbf{C}_{s_1}^{b_1,t_1}\{v_{b_2-s_2+2}\} \\ \vdots & \vdots & \vdots \\ \mathbf{C}_{s_1}^{b_1,t_1}\{v_{t_2}\} & \ldots & \mathbf{C}_{s_1}^{b_1,t_1}\{v_{t_2-s_2+1}\} \end{pmatrix}}_{s_2 \text{ blocks}} \tag{1}$$

and

$$\mathbf{C}_s^{b,t}\{v_j\} = \begin{pmatrix} v(b, j) & v(b-1, j) & \ldots & v(b-s+1, j) \\ v(b+1, j) & v(b, j) & \ldots & v(b-s+2, j) \\ \vdots & \vdots & \vdots & \vdots \\ v(t, j) & v(t-1, j) & \ldots & v(t-s+1, j) \end{pmatrix},$$

where $v(i, j) = 0$ for $i < 1 \vee i > s_1 \vee j < 1 \vee j > s_2$.

III. Problem formulation

We first define the single-input multiple-output degradation model in the discrete domain $\mathbb{N}^2$ as follows. Suppose that an original (input) image $u(x)$ has support $1 \le x \le S_u$. The input image propagates through K different channels that behave as linear filters each with a finite impulse response (blurs) h_k, $k \in \{1, \ldots, K\}$. Let the maximum support of the blurs be S_h. In each channel, the image is further degraded with

additive white Gaussian noise (AWGN) n_k of zero mean and variance σ^2 and shifted by $t_k \in \mathbb{N}^2$, $t_k \geq 0$. Let S_t denote the maximum observed shift. On the output, we receive degraded and shifted images $z_k(x)$ with minimum support $1 \leq x \leq S_z$, where $S_z = S_u - S_h - S_t + 1$. The whole model can be expressed as

$$z_k(x) = \sum_{1 \leq y \leq S_u - S_h + 1} \delta_{t_k}(x - y + S_t + 1) \sum_{1 \leq z \leq S_u} h_k(y - z + S_h) u(z) + n_k(x)\,,$$

where $x, y, z \in \mathbb{N}^2$ and δ_{t_k} is a discrete delta function at $S_t - t_k + 1$. By concatenating columns of the images, we can rewrite the previous equation in matrix-vector notation as

$$\mathbf{z}_k = \mathbf{T}_k \mathbf{H}_k \mathbf{u} + \mathbf{n}_k\,,$$

where $\mathbf{z}_k$, $\mathbf{u}$ and $\mathbf{n}_k$ are corresponding column image vectors. $\mathbf{T}_k = \mathbf{C}_{S_u - S_h + 1}^{S_t + 1, S_u - S_h + 1}\{\delta_{t_k}\}$ is of size $\prod(S_u - S_h - S_t + 1) \times \prod(S_u - S_h + 1)$ and $\mathbf{H}_k = \mathbf{C}_{S_u}^{S_h, S_u}\{h_k\}$ is of size $\prod(S_u - S_h + 1) \times \prod S_u$. Both matrices are constructed according to (1) and perform "cropped" convolution, i.e. the support of the result is only a part of the full convolution support. It is easy to verify that the matrix product $\mathbf{T}_k \mathbf{H}_k = \mathbf{G_k}$ defines cropped convolution with a mask $g_k(x) = h_k(x - t_k)$ of size $S_g = S_h + S_t$. This mask is a shifted version of the original blur h_k. By concatenating the output vectors $\mathbf{z} \equiv [\mathbf{z}_1^T, \dots \mathbf{z}_K^T]^T$ and the shifted blur vectors $\mathbf{g} \equiv [\mathbf{g}_1^T, \dots, \mathbf{g}_K^T]^T$, the multichannel model can be rewritten in two equivalent forms

$$\mathbf{z} = \mathbf{G}\mathbf{u} + \mathbf{n} = \mathbf{U}\mathbf{g} + \mathbf{n}\,, \tag{2}$$

where $\mathbf{G} \equiv [\mathbf{G}_1^T, \dots, \mathbf{G}_K^T]^T$, $\mathbf{n} \equiv [\mathbf{n}_1^T, \dots, \mathbf{n}_K^T]^T$, and $\mathbf{U}$ is a block–diagonal matrix with K blocks each performing convolution with the image u, i.e.

$$\mathbf{U} \equiv \underbrace{\begin{pmatrix} \mathbf{C}_{S_g}^{S_g, S_u}\{u\} & \dots & \mathbf{0} \\ \vdots & \ddots & \vdots \\ \mathbf{0} & \dots & \mathbf{C}_{S_g}^{S_g, S_u}\{u\} \end{pmatrix}}_{K \text{ blocks}}.$$

We have obtained a standard multichannel convolution model and all conclusions for blur restoration in [4] and [5] apply also to our shifted version. When noise is omitted, it follows from (2) that the "cropped" convolution matrix $\mathcal{Z}_k \equiv \mathbf{C}_{S_{\bar{g}}}^{S_{\bar{g}}, S_z}\{z_k\}$ for some arbitrary support $S_{\bar{g}}$ is given by

$$\mathcal{Z}_k = \mathcal{U}\mathcal{G}_k\,, \tag{3}$$

where $\mathcal{U} \equiv \mathbf{C}_{S_g + S_{\bar{g}} - 1}^{S_g + S_{\bar{g}} - 1, S_u}\{u\}$ and $\mathcal{G}_k \equiv \mathbf{C}_{S_{\bar{g}}}^{1, S_g + S_{\bar{g}} - 1}\{g_k\}$. The above equality determines the rank property of $\mathcal{Z}_k$ and is utilized in the following lemma.

First, we recall an important definition from [5]. Let $\tilde{h}_k(z_1, z_2)$ denotes the 2D z-transform of the blur h_k. The polynomials $\{\tilde{h}_k(z_1, z_2)\}$ are called "weakly coprime" if their only common factor is a scalar constant.

Lemma 1: Suppose that $K \geq 2$, $\{\tilde{h}_k(z_1, z_2)\}_{k=1}^K$ are weakly coprime, $\mathcal{U}$ in (3) has full column rank and the noise term is not present in (2). Then all solutions $\{\bar{\mathbf{g}}_k\}$ to

$$\mathcal{Z}_i \bar{\mathbf{g}}_j - \mathcal{Z}_j \bar{\mathbf{g}}_i = \mathbf{0}\,, \quad 1 \leq i < j \leq K \tag{4}$$

have the form

$$\bar{\mathbf{g}}_k = \begin{cases} \mathbf{C}_{S_g}^{1, S_{\bar{g}}}\{f\}\mathbf{g}_k & \text{if } S_{\bar{g}} \geq S_h + S_t\,, \\ \alpha \mathbf{g}_k & \text{if } S_{\bar{g}} = S_h + S_t\,, \\ \emptyset & \text{otherwise,} \end{cases}$$

where f is some spurious factor of size $S_{\bar{g}} - S_h - S_t + 1$ and α is some scalar.

The proof is similar in nature to the proof given in [4] except that S_t is included in size constraints as discussed below. The above lemma states that in the noiseless case, if the estimated blur size $S_{\bar{g}}$ is equal to the sum of the maximum size of the original blurs S_h and the maximum shift S_t, then the true shifted blurs can be recovered precisely except to some scalar factor. This magnitude ambiguity can be resolved by stipulating, e.g., $\sum_x h_k(x) = 1$, which is a standard energy preserving assumption. For oversized $S_{\bar{g}}$, the solutions lie in a space that contains the original blurs but the dimensionality of the solution space is proportional to the degree of the oversize. The first assumption that the blurs are weakly coprime is satisfied for many practical cases, since the necessary channel disparity is mostly guaranteed by the nature of the acquisition scheme and random processes therein. Refer to [4] for a relevant discussion. The second assumption of full column rank is also a mild one. For generic u, the matrix $\mathcal{U}$ has full column rank provided that it has more rows than columns. Let us assume that the blur size is correctly estimated, i.e. $S_{\bar{g}} = S_g$, then $\mathcal{U}$ is of size $\prod(S_u - 2(S_g + 1)) \times \prod(2S_g - 1)$ from which follows a size constraint $\prod(S_u - 2(S_h + S_t + 1)) \geq \prod(2(S_h + S_t) - 1)$. Generally, u is much bigger than h and the size constraint is violated only if the channel shift is for example $S_t > \frac{S_u + 3}{4} - S_h$. It follows that $\mathcal{U}$ does not have certainly full column rank if $S_t > S_u/4$.

There are $K(K-1)/2$ equations in (4) and after stacking them into one system, we get

$$\mathbf{Z}\bar{\mathbf{g}} = \mathbf{0}\,, \tag{5}$$

where $\bar{\mathbf{g}} \equiv [\bar{\mathbf{g}}_1^T, \dots, \bar{\mathbf{g}}_K^T]^T$,

$$\mathbf{Z} \equiv \begin{pmatrix} \mathbf{Z}_1 \\ \vdots \\ \mathbf{Z}_{K-1} \end{pmatrix}, \qquad \mathbf{Z}_i \equiv \underbrace{\begin{pmatrix} \mathbf{0} & \dots & \mathbf{0} & \mathcal{Z}_{i+1} & \dots & -\mathcal{Z}_i & \dots \\ \vdots & \ddots & \vdots & \vdots & \ddots & \vdots & \vdots \\ \mathbf{0} & \dots & \mathbf{0} & \mathcal{Z}_K & \dots & \dots & -\mathcal{Z}_i \end{pmatrix}}_{\substack{i-1 \text{ blocks} \\ \qquad}} \underbrace{\qquad\qquad}_{K-i+1 \text{ blocks}} \tag{6}$$

for $i = 1, \dots, K-1$. From Lemma 1 follows that the dimension of the null space of $\mathbf{Z}$ is $\prod(S_{\bar{g}} - S_g + 1)$. In the presence of noise, the left-hand side of (5) is not zero anymore but is proportional to the noise level.

Adopting a stochastic approach, the minimization problem can be formulated as a maximum a posterior (MAP) estimation. We assume that the images $\mathbf{u}$, $\mathbf{g}$ and $\mathbf{z}$ are random vector fields with given probability density functions (pdf) $p(\mathbf{u})$, $p(\mathbf{g})$ and $p(\mathbf{z})$, respectively, and we look for such

realizations of $\mathbf{u}$ and $\mathbf{g}$ which maximize the a posterior probability $p(\mathbf{u},\mathbf{g}|\mathbf{z})$. We assume that $\mathbf{u}$ and $\mathbf{h}$ are uncorrelated then, according to the Bayes rule, the relation between a priori densities $p(\mathbf{u})$, $p(\mathbf{g})$ and the a posterior density is $p(\mathbf{u},\mathbf{g}|\mathbf{z}) = p(\mathbf{z}|\mathbf{u},\mathbf{g})p(\mathbf{u})p(\mathbf{g})/p(\mathbf{z})$. The pdf $p(\mathbf{z})$ is a constant and can be thus omitted. The conditional pdf $p(\mathbf{z}|\mathbf{u},\mathbf{g})$ follows from our model (2) and from our assumption of AWGN, i.e.,

$$p(\mathbf{z}|\mathbf{u},\mathbf{g}) \propto \exp\left\{-\frac{1}{2\sigma^2}(\mathbf{z}-\mathbf{G}\mathbf{u})^T(\mathbf{z}-\mathbf{G}\mathbf{u})\right\}. \quad (7)$$

A. A priori distribution of the original image

The necessity of meaningful a priori probabilities becomes often Achilles' heel of Bayesian approaches. Several different forms of the image a priori probabilities were proposed in the literature. Some are suitable only for a specific class of images and others are more general. The classical general form chooses the Laplacian operator as the inverse of the covariance matrix of u, i.e., $p(\mathbf{u}) \propto \exp(\mathbf{u}^T\nabla^2\mathbf{u})$, where ∇^2 denotes the discrete Laplacian operator. Apart from easy implementation, this pdf is not suitable for the a priori model, since it prefers smooth functions without any discontinuities. On real images, object edges create sharp steps that appear as discontinuities in intensity functions. Geman et al. [10] thus proposed a more sophisticated model with a "line process" which keeps track of edge locations. Similar results were obtained for the Mumford-Shah functional [11] that introduces a discontinuity set on which the image function is allowed to have an infinite image gradient. It is the space of bounded variation (BV) functions that is widely accepted as a proper setting for real images. This has been proved many times [3] by demonstrating very good anisotropic denoising properties of the total variation semi-norm $TV(u) = \int |Du(x)|dx$ that is finite only in the BV space. Here, Du denotes the distributional gradient of u. Since TV is highly nonlinear and not continuous at $Du(x) = 0$, a special attention must be paid to its discretization and several relaxed linearization schemes were proposed. We follow the half-quadratic regularization scheme in [12] that introduces an auxiliary variable. First, let us recall:

Lemma 2: For every $x \in \mathbb{R}$, $x \neq 0$

$$|x| = \min_{v>0}\left(\frac{v}{2}x^2 + \frac{1}{2v}\right),$$

the minimum is reached for $v = 1/|x|$.

The a priori distribution of the original image can be thus expressed as

$$p(\mathbf{u},v) \propto \exp\Big\{\frac{1}{2}\sum_{i,j} v(i+\tfrac{1}{2},j)|u(i+1,j)-u(i,j)|^2 + v(i,j+\tfrac{1}{2})|u(i,j+1)-u(i,j)|^2\Big\} \equiv \exp\left\{-\frac{1}{2}\mathbf{u}^T\mathbf{L}(v)\mathbf{u}\right\}, \quad (8)$$

where v is the auxiliary flux variable similar to Geman's line process. It is indexed $(i\pm\frac{1}{2}, j\pm\frac{1}{2})$ instead of (i,j) to underline that it denotes the edge strength between point (i,j) and its neighbors $(i\pm1, j\pm1)$. Matrix $\mathbf{L}(v)$ is positive semidefinite constructed by v and performs shift-variant convolution with v. To avoid division by zero and in accordance with the above lemma,

$$v(i\pm\tfrac{1}{2}, j\pm\tfrac{1}{2}) = \begin{cases} \frac{1}{|u(i\pm1,j\pm1)-u(i,j)|} & \text{if } |u(i\pm1,j\pm1)-u(i,j)| > \epsilon \\ \frac{1}{\epsilon} & \text{otherwise,} \end{cases} \quad (9)$$

where ϵ is the relaxation parameter. Note that in relatively flat regions, $|Du(x)| \leq \epsilon$, $\mathbf{L}(v)$ becomes the Laplacian operator. In regions with high image gradient, $|Du(x)| > \epsilon$, $\mathbf{u}^T\mathbf{L}(v)\mathbf{u}$ approximates the TV semi-norm of the image $\mathbf{u}$.

B. A priori distribution of blurs

The a priori distribution $p(\mathbf{g})$ can be derived directly from the multichannel model. The Bayes rule states that $p(\mathbf{g}) = p(\mathbf{g}|\mathbf{z})p(\mathbf{z})/p(\mathbf{z}|\mathbf{g})$, where $p(\mathbf{z})$ is a constant and can be thus dropped. To proceed, the conditional probabilities $p(\mathbf{g}|\mathbf{z})$ and $p(\mathbf{z}|\mathbf{g})$ are necessary to derive. After substituting for $\mathbf{Z}$ from (2), we see that $E\{\|\mathbf{Z}\mathbf{g}\|^2\} = \sigma^2\,\mathrm{Tr}(\mathcal{G}\mathcal{G}^T)$, where $\mathcal{G}$ is defined as $\mathbf{Z}$ in (6) with $\mathbf{C}_{S_z}^{S_g,S_z}\{g_i\}$ substituted for $\mathcal{Z}_i$. The conditional pdf $p(\mathbf{g}|\mathbf{z})$ is then given by

$$p(\mathbf{g}|\mathbf{z}) \propto \exp\Big\{-\frac{1}{2\sigma^2}\mathbf{g}^T\mathbf{Z}^T(\mathcal{G}\mathcal{G}^T)^{-1}\mathbf{Z}\mathbf{g}\Big\}. \quad (10)$$

The main difficulty arising here is the covariance matrix $\mathcal{G}\mathcal{G}^T$ that totally depends on the blurs $\mathbf{g}$, which are not known in advance. One way would be to use an iterative algorithm and construct $\mathcal{G}$ from $\mathbf{g}$ of the previous iteration. Such kind of the iterative maximization of $p(\mathbf{g}|\mathbf{z})$ w.r.t. $\mathbf{g}$ is in accord with the IQML algorithm in [4]. Our numerical experiments have shown, however, that the covariance matrix can be approximated by a constant diagonal matrix $\mathcal{D}$ such that $\mathrm{Tr}(\mathcal{D}) = \mathrm{Tr}(\mathcal{G}\mathcal{G}^T)$, i.e. $\mathcal{D} = (2/K)E\{\|\mathbf{g}\|^2\}\mathbf{I} = (2/K)E\{\|\mathbf{h}\|^2\}\mathbf{I}$. This greatly simplifies the calculation and does not inflict the restoration. The expected value of $\|\mathbf{h}\|^2$ is not known in advance, but a good approximation can be given. If energy preserving assumption, $\sum_x h_k(x) = 1$, and positiveness, $h_k \geq 0$, are satisfied then $\frac{K}{\prod S_h} \leq \|\mathbf{h}\|^2 \leq K$ and we use the bottom limit for $E\{\|\mathbf{h}\|^2\}$.

The conditional pdf $p(\mathbf{z}|\mathbf{g})$ can be expressed as $p(\mathbf{z}|\mathbf{g}) = \int p(\mathbf{z}|\mathbf{u},\mathbf{g})p(\mathbf{u})\,d\mathbf{u}$. To obtain an analytical solution, we must assume that the matrix $\mathbf{L}(v)$ in $p(\mathbf{u})$ is constant and not dependent on v. Therefore, we approximate $\mathbf{L}$ with the discrete Laplacian operator $\frac{1}{\epsilon}\nabla^2$. The analytical result is summarized in the following lemma.

Lemma 3: For the model in (2), suppose that $p(\mathbf{n}) = k_n\exp(-\frac{1}{2\sigma^2}\mathbf{n}^T\mathbf{n})$, $p(\mathbf{u}) = k_u\exp(-\frac{1}{2}\mathbf{u}^T\mathbf{L}\mathbf{u})$ and $p(\mathbf{h})$ are uncorrelated, then

$$p(\mathbf{z}|\mathbf{g}) = k\exp\Big\{-\frac{1}{2}\mathbf{z}^T\Big[\frac{1}{\sigma^2}\mathbf{I} - \frac{1}{\sigma^4}\mathbf{G}(\mathbf{A}^T\mathbf{A})^{-1}\mathbf{G}^T\Big]\mathbf{z}\Big\}\times \sqrt{\frac{2\pi^{S_u^1 S_u^2}}{\det(\mathbf{A}^T\mathbf{A})}}, \quad (11)$$

where $\mathbf{A}^T\mathbf{A} = \frac{1}{\sigma^2}\mathbf{G}^T\mathbf{G} + \mathbf{L}$ and k is the appropriate normalization constant.

The proof is carried out directly by substituting for $p(\mathbf{n})$ and $p(\mathbf{u})$ in relevant equations.

It is easy to verify that the exponential term in (11) is extremely flat w.r.t. $\mathbf{g}$ and can be thus regarded as a constant term. Finally, after substituting $\mathcal{D}$ for $\mathcal{G}\mathcal{G}^T$, we obtain from (10) and (11) that

$$p(\mathbf{g}) \propto \exp\Big\{-\frac{K}{4\sigma^2\|\mathbf{h}\|^2}\mathbf{g}^T\mathbf{Z}^T\mathbf{Z}\mathbf{g}\Big\}\sqrt{\det(\mathbf{A}^T\mathbf{A})}\,. \quad (12)$$

C. AM–MAP algorithm

The a posterior pdf $p(\mathbf{u},\mathbf{g}|\mathbf{z})$ is composed of (7), (8), (12) and turns out to be

$$p(\mathbf{u},\mathbf{g}|\mathbf{z}) \propto \exp\Big\{-\frac{1}{2}\Big(\frac{1}{\sigma^2}(\mathbf{z}-\mathbf{G}\mathbf{u})^T(\mathbf{z}-\mathbf{G}\mathbf{u})+ \mathbf{u}^T\mathbf{L}(v)\mathbf{u}+\frac{K}{2\sigma^2\|\mathbf{h}\|^2}\mathbf{g}^T\mathbf{Z}^T\mathbf{Z}\mathbf{g}\Big)\Big\}\sqrt{\det(\mathbf{A}^T\mathbf{A})}$$

The MAP estimation is equivalent to minimizing $E(\mathbf{u},\mathbf{g}) = -\log(p(\mathbf{u},\mathbf{g}|\mathbf{z}))$, i.e.

$$E(\mathbf{u},\mathbf{g}) = \frac{1}{\sigma^2}(\mathbf{z}-\mathbf{G}\mathbf{u})^T(\mathbf{z}-\mathbf{G}\mathbf{u}) + \mathbf{u}^T\mathbf{L}(v)\mathbf{u}+ \frac{K}{2\sigma^2\|\mathbf{h}\|^2}\mathbf{g}^T\mathbf{Z}^T\mathbf{Z}\mathbf{g} - \log(\det(\mathbf{A}^T\mathbf{A}))\,. \quad (13)$$

To find a minimizer of the energy function E, we perform alternating minimizations of E over $\mathbf{u}$ and $\mathbf{g}$. The advantage of this scheme lies in its simplicity. Each term in (13), except the logarithmic one, is convex (but not necessarily strictly convex, especially, when $\mathbf{g}$ is oversized). The derivatives w.r.t. $\mathbf{u}$ and $\mathbf{g}$ can be easily calculated for each except again the logarithmic term. However, if $\mathbf{G}$ and $\mathbf{L} = (1/\epsilon)\nabla^2$ are approximated by circulant-block-circulant (CBC) matrices, we conclude that

$$\nabla_{g_i}\Big(\log(\det(\mathbf{A}^T\mathbf{A}))\Big) = \frac{2}{\sigma^2}\mathcal{F}^{-1}\left\{\frac{\mathcal{F}\{g_i\}}{\frac{\sum_{k=1}^K\|\mathcal{F}\{g_k\}\|^2}{\sigma^2}+\Lambda}\right\},$$
$$\mathbf{r} = [\nabla_{g_1}^T,\ldots,\nabla_{g_K}^T]^T,$$

where Λ are the eigenvalues of approximated CBC $\mathbf{L}$. This term closely resembles the MC Wiener filter and Λ prevents division by zero. In summary, the AM–MAP algorithm consists of

$$\begin{aligned}\mathbf{g}^{m+1} &= \arg\min_{\mathbf{g}} E(\mathbf{u}^m,\mathbf{g}) \Leftrightarrow \\ &\quad (\mathbf{U}^T\mathbf{U}+\frac{K}{2\|\mathbf{h}\|^2}\mathbf{Z}^T\mathbf{Z})\mathbf{g}+\mathbf{r} = \mathbf{U}^T\mathbf{z}\,, \\ \mathbf{u}^{m+1} &= \arg\min_{\mathbf{u}} E(\mathbf{u},\mathbf{g}^{m+1}) \Leftrightarrow \\ &\quad (\mathbf{G}^T\mathbf{G}+\sigma^2\mathbf{L}(v))\mathbf{u} = \mathbf{G}^T\mathbf{z}\,.\end{aligned} \quad (14)$$

In each step, the flux variable v is updated according to (9).

Our AM approach is a variation on the steepest-descent algorithm. The search space is a concatenation of the blur subspace and the image subspace. The algorithm first descends in the blur subspace and after reaching the minimum, i.e., $\nabla_{\mathbf{g}}E = 0$, it advances in the image subspace in the direction $\nabla_{\mathbf{u}}E$ orthogonal to the previous one, and this scheme repeats. The preconditioned conjugate gradient (PCG) method is used to solve the individual equations. E as a function of both variables $\mathbf{u}$ and $\mathbf{g}$ is not convex. Therefore, we cannot guarantee, in general, that the global minimum is reached by the AM–MAP algorithm. Nevertheless, our experiments have shown good convergence properties even for the oversized blurs. We also assume that the noise variance σ^2 is known. If this is not the case, the noise variance can be assessed by standard noise estimation methods or an approach of "trial and error" can be considered. The impact of wrong σ^2 can be easily observed. If the parameter is too small, i.e. we assume less noise, the restoration process begins to amplify noise in the image. If the parameter is too big, the restoration process starts to segment the image.

IV. Oversized blurs

It is difficult to analyze global convergence properties of the algorithm (14) due to the nonlinear term $\mathbf{L}(v)$. Chan et al. in [13] transformed a similar alternating minimization problem into the Fourier domain and performed the analysis there. Sadly, this approach is false in our case since the support constraint of the blurs is lost in the Fourier domain and therefore blind deconvolution is very "loose" in the Fourier domain. It means that any image u which in the z-transform splits only into two factors, $\tilde{u} = \tilde{u}_1\tilde{u}_2$, has infinite number of factors in the Fourier domain.

We have run a series of experiments on simulated data with an incorrectly estimated blur size. A standard 128×128 "Lena" image in Fig. 2 was degraded with three random blurs of size 5×5 and with additive Gaussian noise of SNR = 20, 30, 40, 50dB. (Recall that SNR decreases as noise variance increases.) The original image was recovered from each image triplet using the alternating minimization algorithm with the blur size set to 5×5, 6×6, 7×7 and 8×8, respectively. The percentage mean squared error of the estimated image $\bar{\mathbf{u}}$,defined as $\mathrm{PMSE}(\bar{\mathbf{u}}) = 100\|\bar{\mathbf{u}}-\mathbf{u}\|/\|\mathbf{u}\|$, was used as the evaluation measure at each iteration. Calculated PMSE's are summarized in Fig. 1. We can see that the slope of PMSE tends to flatten as the blur size increases. It follows from Lemma 1 that rank of $\mathbf{Z}$ decreases as the order of oversize grows. In the noisy case, this corresponds to an increasing number of eigenvalues of $\mathbf{Z}$ bellow the noise level, which implies the slower convergence rate of the CG method. We observe even slower convergence rate for less noisy images (SNR = 50dB) since here the eigenvalues cluster close to zero.

V. Shift-invariant restoration

The first experiment demonstrates the capability of the AM–MAP algorithm to recover the original image from two degraded and shifted versions thereof, when the maximum shift between any two channels is known. The 128×128 "Lena" image in Fig. 2 was degraded with two 5×5 blurs. One blurred image was shifted by 10×20 pixels and then both images were cropped to the same size; see Fig. 3. The AM algorithm was initialized with the correctly estimated blur size 15×25. The restored image and blurs are shown in Fig. 4. The blurs are perfectly recovered and properly shifted. The restored image matches the original one, showing only minor

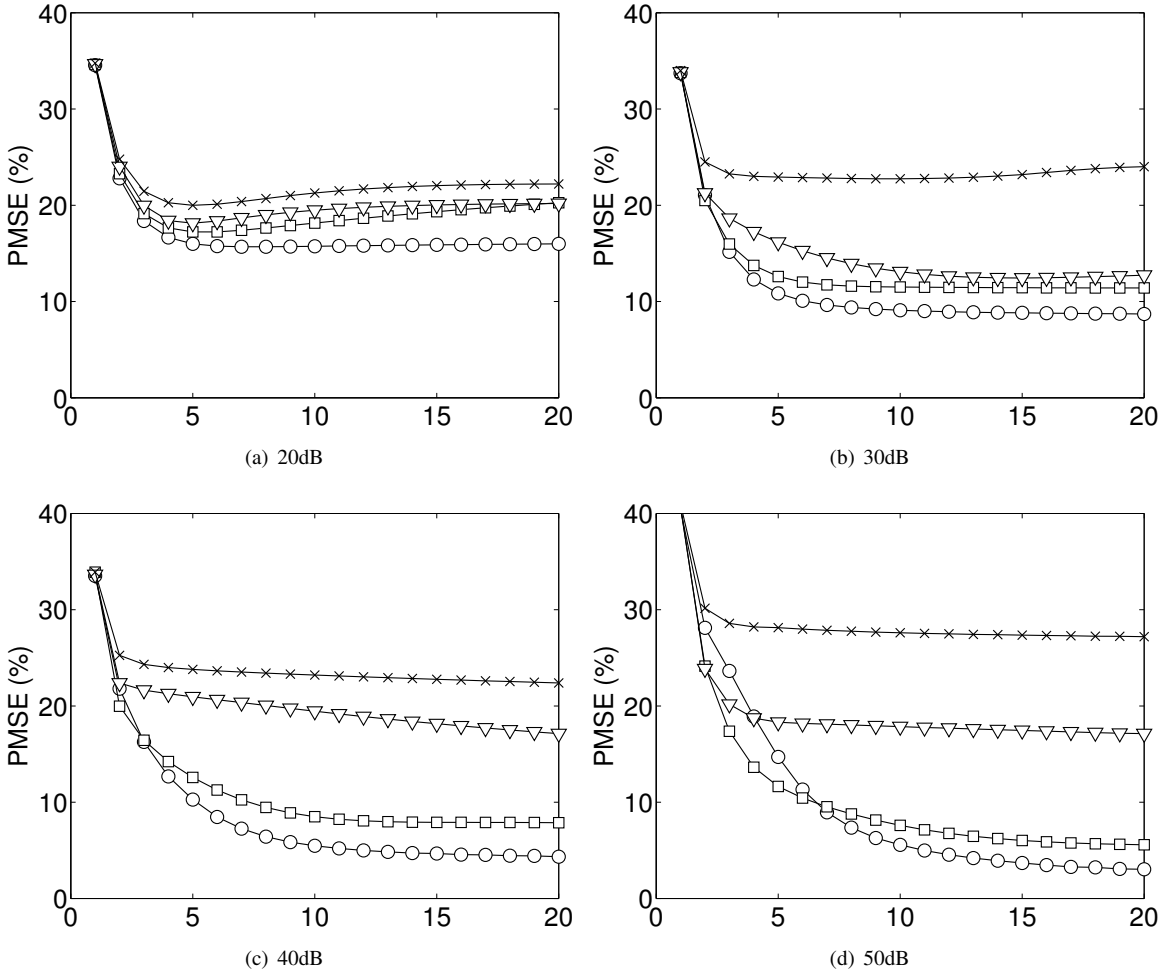

(a) 20dB (b) 30dB

(c) 40dB (d) 50dB

Fig. 1. PMSE of the "Lena" image calculated at each iteration step. The "Lena" image was degraded with three random blurs of size 5×5 and with AWGN of SNR (a) 20dB, (b) 30dB, (c) 40dB and (d) 50dB. The AM algorithm was executed with the estimated blur size ($\bigcirc$) 5×5 (correct size), ($\square$) 6×6, ($\triangledown$) 7×7 and ($\times$) 8×8

artifacts close to the borders where only data from one channel were available. The same experiment was conducted again but Gaussian noise SNR = 30 dB was added to the blurred and shifted input images in Fig. 3. Obtained results in Fig. 5 illustrate satisfying restoration.

We have also compared the performance of the AM–MAP algorithm with the performance of Pai's method [8] for different noise levels. The Pai approach directly recovers the original image by calculating the maximum singular vector of a special matrix. The *QR decomposition* is necessary for the construction of this matrix and the *power method* (or any other iterative method for eigenvector computation) is used to find the maximum singular vector, i.e the original image. Although the Pai method is not iterative in its definition, it requires numerical iterative methods and thus approaches the complexity of our inherently iterative algorithm. We used four randomly generated 3×3 blurs to obtain four blurred "Lena" images. The images were then mutually translated so that centers of the images were in corners of a 5×5 square. Noise was added with SNR = 10, 20, 30, 40 and 50 dB, respectively. The maximum shift and the size of blurs were assumed to be known and therefore both methods were initialized with the correct blur size 8×8. For each SNR, the experiment was repeated with different blurs 10 times and stopped after 50 iterations in the AM–MAP case. The mean PMSE and standard deviation was calculated over these 10 estimated images and plotted in Fig. 6. Clearly, the AM–MAP performs better then the Pai method for every SNR.

To evaluated the performance of the AM–MAP algorithm with respect to the channel misalignment, a different experiment was conducted. Degraded images were prepared in similar fashion as in the previous experiment but this time the maximum translation between any two channels varied from 0 to 5×5 pixels to simulate inaccurate registration. For each shift, the experiment was repeated 10 times with different blurs and was every time initialized to 8×8 blur size. The calculated mean PMSE and standard deviation is given in Figs. 7 and 8. For low SNR's around 10 and 20 dB, PMSEs are almost constant, which demonstrates a very good stability of the algorithm with respect to the mask overestimation. In the case of high SNR's, see Fig. 8, we can observe a steady growth of the restoration error as the shift increases and then a dramatic performance gain for shift 5. This sharp error decrease is due to much better convergence of the algorithm if the blur size is

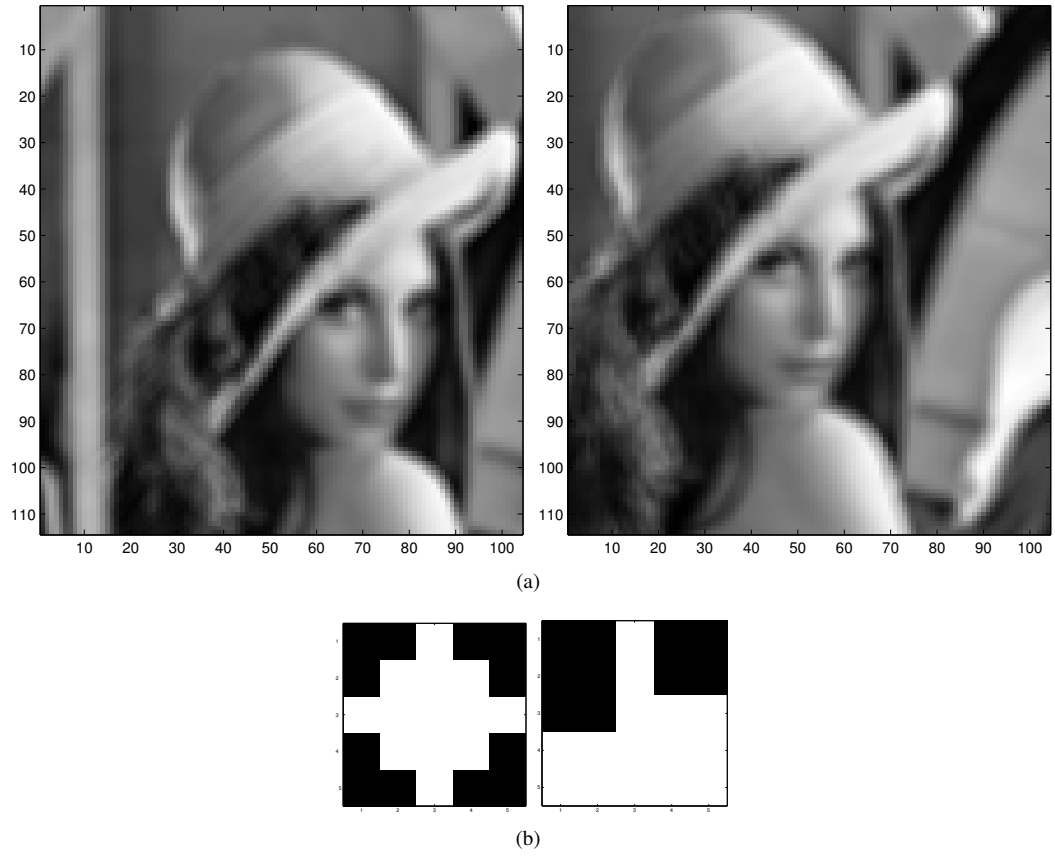

Fig. 3. Input channels: (a) "Lena" images degraded with two 5×5 blurs in (b) . Mutual translation between the images is 10×20 pixels.

Fig. 2. The original "Lena" image 128×128.

correctly estimated, which, in our case, corresponds to shift 5. Results for low SNR's in Fig. 7 do not exhibit such dramatic performance gains as the impact of noise prevailed over the blur size overestimation.

Finally, to demonstrate the applicability of the AM–MAP algorithm, we have performed an experiment with real data. This experiment was motivated by many practical situations where we have to handle images degraded by random vibration

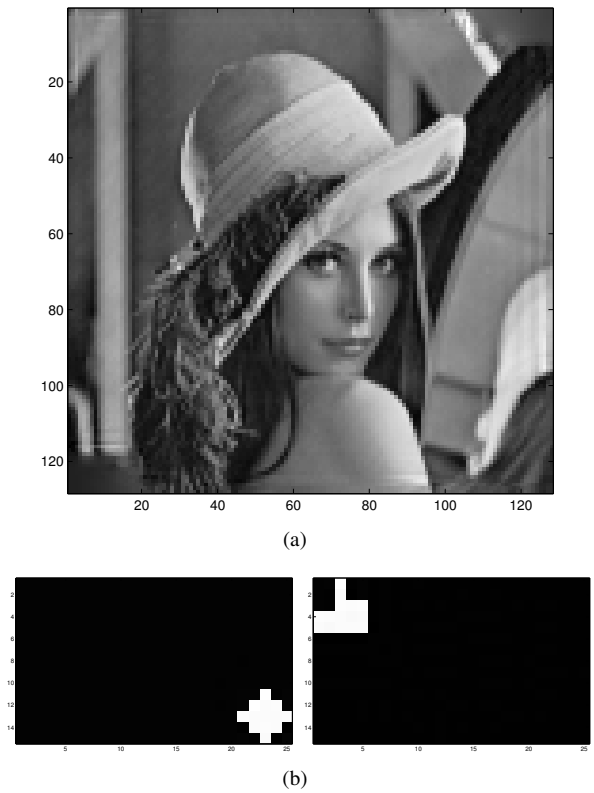

Fig. 4. Perfect noise-free AM restoration: (a) recovered "Lena" image, (b) recovered blurs and 10×20 shift between channels

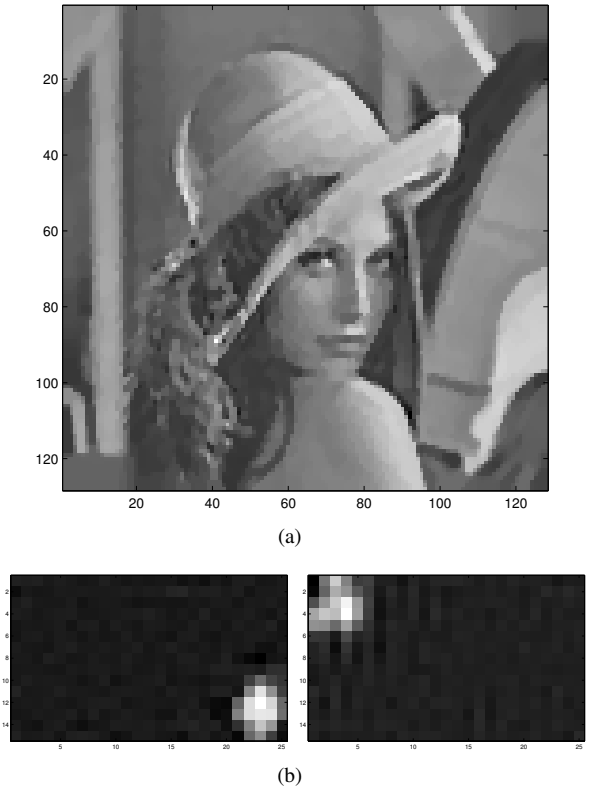

(a)

(b)

Fig. 5. Noisy AM restoration (30dB): (a) recovered "Lena" image, (b) recovered blurs and 10×20 shift between channels

blur. This problem appears frequently in industrial visual inspection when the camera is mounted on a vibrating machine or when a stationary camera monitors vibrating environment. A text label (a part of a standard newspaper page) was attached to a vibrating machine. The label was monitored under poor light conditions by a standard digital camera mounted on a tripod. The camera exposure time was set at $1/15$s which was comparable to the period of irregular vibrations of the machine. Three cropped images of the label acquired with the camera were used as the input channels of AM–MAP; see Fig. 9. Note strong shift blurs due to the machine movement and clear spatial misalignment of the channels. The AM–MAP algorithm was initialized with the blur size 10×10, $\sigma^2 = 0.01$ and $\|\mathbf{h}\|^2 = 0.25$. The reconstructed label and the corresponding blur masks after 20 iterations are shown in Fig. 10. Observe that the restoration is slightly less successful at the image borders, especially close to the top edge, where only data from the third channel were available. We may conclude that the restoration was successful (the text is clearly readable) and that the spatial misalignment inherent to this type of problems poses no threat to proper functionality of the algorithm. Let us recall that no assumption about the shape of the blurring functions and no preprocessing of the input images were employed.

VI. Conclusion

We have developed the iterative algorithm for MC blind deconvolution that searches for the MAP estimator. The prior density functions were derived from the variational integral

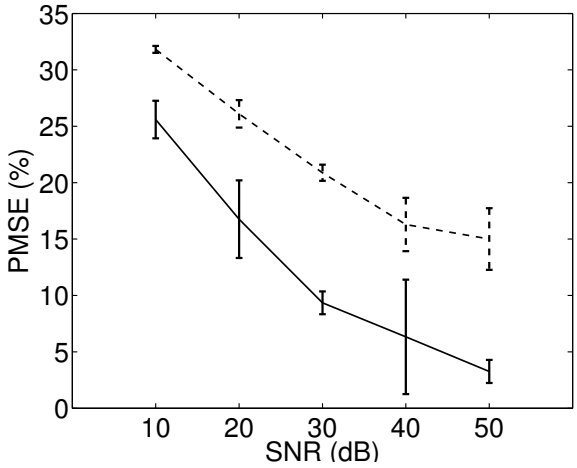

Fig. 6. Comparison of the AM–MAP algorithm (solid) and the Pai method (dashed): Mean PMSE and standard deviation (vertical abscissae) of the restored images over 10 different degradations and for different SNR.

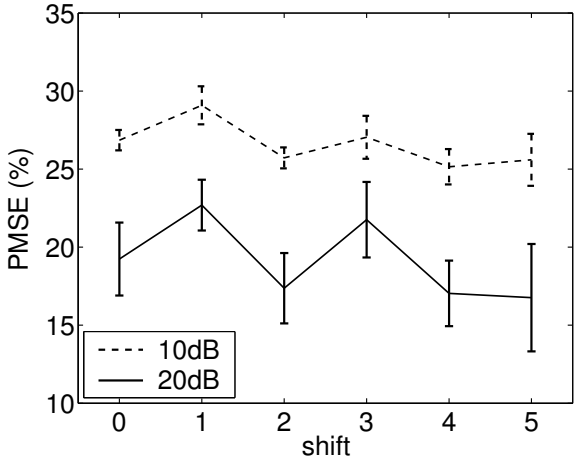

Fig. 7. AM-MAP algorithm performance on misaligned channels: Mean PMSE and standard deviation (vertical abscissae) of restored images over 10 different degradations for a different degree of channel misalignment and SNR.

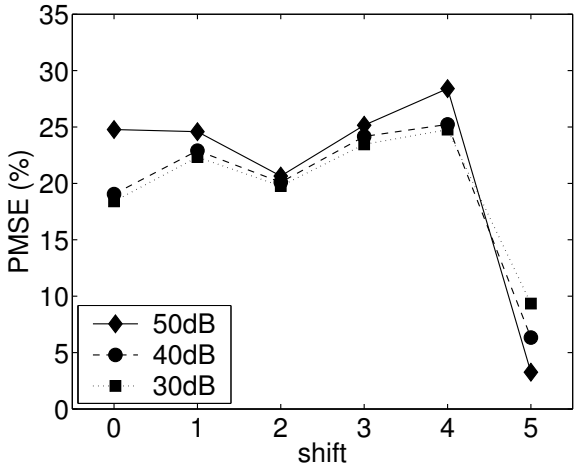

Fig. 8. AM-MAP algorithm performance on misaligned channels: Mean PMSE of restored images over 10 different degradations for a different degree of channel misalignment and SNR.

Fig. 9. Real data experiment: Three consecutive acquisitions of a text label attached to a vibrating machine. The images are cropped to 100×200 size. Shift blurs and spatial misalignment of the images are clearly visible.

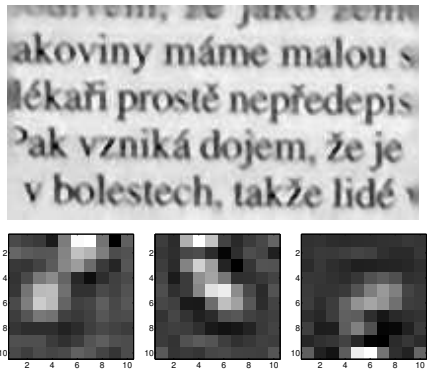

Fig. 10. Real data experiment: Reconstructed part of the label and the corresponding blurs (magnified) using the AM–MAP algorithm. The irregular vibration of the machine is well preserved in the blurs.

defined on bounded variation functions and from the mutual relation of weakly coprime channels. The restoration is regularized with an anisotropic term for edge preservation and performs well on heavily degraded images with high SNR and shows better performance then the most recent multichannel method. We have also shown that the inaccurate registration of channels can be alleviated by properly overestimating the size of blurs. All previously published MC blind deconvolution methods assumed perfectly registered channels. To our knowledge, this is the only method dealing explicitly with misregistration of images in the multichannel framework and providing a successful solution to this problem.

REFERENCES

[1] M. Banham and A. Katsaggelos, "Digital image restoration," *IEEE Signal Processing Magazine*, vol. 14, no. 2, pp. 24–41, Mar. 1997.

[2] D. Kundur and D. Hatzinakos, "Blind image deconvolution," *IEEE Signal Processing Magazine*, vol. 13, no. 3, pp. 43–64, May 1996.

[3] L. Rudin, S. Osher, and E. Fatemi, "Nonlinear total variation based noise removal algorithms," *Physica D*, vol. 60, pp. 259–268, 1992.

[4] G. Harikumar and Y. Bresler, "Perfect blind restoration of images blurred by multiple filters: Theory and efficient algorithms," *IEEE Trans. Image Processing*, vol. 8, no. 2, pp. 202–219, Feb. 1999.

[5] G. Giannakis and R. Heath, "Blind identification of multichannel FIR blurs and perfect image restoration," *IEEE Trans. Image Processing*, vol. 9, no. 11, pp. 1877–1896, Nov. 2000.

[6] G. Harikumar and Y. Bresler, "Exact image deconvolution from multiple FIR blurs," *IEEE Trans. Image Processing*, vol. 8, pp. 846–862, June 1999.

[7] H.-T. Pai and A. Bovik, "Exact multichannel blind image restoration," *IEEE Signal Processing Letters*, vol. 4, no. 8, pp. 217–220, Aug. 1997.

[8] ——, "On eigenstructure-based direct multichannel blind image restoration," *IEEE Trans. Image Processing*, vol. 10, no. 10, pp. 1434–1446, Oct. 2001.

[9] F. Šroubek and J. Flusser, "Multichannel blind iterative image restoration," *IEEE Trans. Image Processing*, to appear, accepted in 2003.

[10] D. Geman and G. Reynolds, "Constrained restoration and the recovery of discontinuities," *IEEE Trans. Pattern Anal.*, vol. 14, no. 3, pp. 367–383, Mar. 1992.

[11] D. Mumford and J. Shah, "Optimal approximation by piecewise smooth functions and associated variational problems," *Comm. Pure Appl. Math.*, vol. 42, pp. 577–685, 1989.

[12] A. Chambolle and P. Lions, "Image recovery via total variation minimization and related problems," *Numer. Math.*, vol. 76, no. 2, pp. 167–188, Apr. 1997.

[13] T. Chan and C. Wong, "Convergence of the alternating minimization algorithm for blind deconvolution," *Linear Algebra Appl.*, vol. 316, no. 1-3, pp. 259–285, Sept. 2000.

Filip Šroubek received the B.Sc. and M.Sc. degrees in computer science from the Czech Technical University, Prague, Czech Republic in 1996 and 1998, respectively, and is currently a Ph.D. candidate in computer science at the Charles University, Prague, Czech Republic.

Since 1999, he has been with the Institute of Information Theory and Automation, Academy of Sciences of the Czech Republic, Prague. Since 2000, he has been with the Institute of Radiotechnique and Electronics, Academy of Sciences of the Czech Republic, Prague, Czech Republic.

His current research interests include all aspects of digital image processing and pattern recognition, particularly multichannel blind deconvolution, image denoising, image registration, and computer simulation and visualization of atomic collision processes.

Jan Flusser received the M.Sc. degree in mathematical engineering from the Czech Technical University, Prague, Czech Republic in 1985, the Ph.D. degree in computer science from the Czechoslovak Academy of Sciences in 1990, and the D.Sc. degree in technical cybernetics in 2001.

Since 1985, he has been with the Institute of Information Theory and Automation, Academy of Sciences of the Czech Republic, Prague. Since 1995, he has been holding the position of a head of Department of Image Processing. Since 1991, he has been also affiliated with the Charles University, Prague, and the Czech Technical University, Prague, where he gives courses on Digital Image Processing and Pattern Recognition.

His current research interests include all aspects of digital image processing and pattern recognition, namely 2-D object recognition, moment invariants, blind deconvolution, image registration and image fusion. He has authored and coauthored more than 80 research publications in these areas.

J. Flusser is a senior member of the IEEE.